Cell

A Role for TFIIIC Transcription Factor Complex in Genome Organization

Ken-ichi Noma,[1] Hugh P. Cam,[1] Richard J. Maraia,[2] and Shiv I.S. Grewal[1,*]
[1] Laboratory of Molecular Cell Biology, National Cancer Institute, National Institutes of Health, Bethesda, MD 20892, USA
[2] Laboratory of Molecular Growth Regulation, National Institute of Child Health and Human Development, National Institutes of Health, Bethesda, MD 20892, USA
*Contact: grewals@mail.nih.gov
DOI 10.1016/j.cell.2006.04.028

SUMMARY

Eukaryotic genome complexity necessitates boundary and insulator elements to partition genomic content into distinct domains. We show that inverted repeat (*IR*) boundary elements flanking the fission yeast mating-type heterochromatin domain contain *B-box* sequences, which prevent heterochromatin from spreading into neighboring euchromatic regions by recruiting transcription factor TFIIIC complex without RNA polymerase III (Pol III). Genome-wide analysis reveals TFIIIC with Pol III at all *tRNA* genes, many of which cluster at pericentromeric heterochromatin domain boundaries. However, a single $tRNA^{phe}$ gene with modest TFIIIC enrichment is insufficient to serve as boundary and requires RNAi-associated element to restrain heterochromatin spreading. Remarkably, we found TFIIIC localization without Pol III at many sites located between divergent promoters. These sites appear to act as chromosome-organizing clamps by tethering distant loci to the nuclear periphery, at which TFIIIC is concentrated into several distinct bodies. Our analyses uncover a general genome organization mechanism involving conserved TFIIIC complex.

INTRODUCTION

Large-scale sequencing of several eukaryotic genomes, including the human genome, has led to detailed insights of genomic content, yielding valuable information about genes and a variety of regulatory elements dispersed across genomes. A major challenge in biological research is to understand the functional organization of genomes that helps translate genetic information into different cell types during development. Epigenetic mechanisms acting at the level of DNA or chromatin packaging proteins (such as DNA methylation and modifications of histones) contribute to how genomes are organized into distinct chromatin domains and utilized in diverse chromosomal processes (Jenuwein and Allis, 2001; Cavalli, 2002). Establishment of individual domains is likely mediated by boundary or insulator elements, specialized DNA sequences separating independently regulated domains that are often marked with distinctive patterns of epigenetic modifications. These elements, known to exist in genomes of diverse species, could shield a particular chromosomal region from positive or negative signals emanating from regulatory elements embedded within neighboring regions (Sun and Elgin, 1999; Bell and Felsenfeld, 2001; Labrador and Corces, 2002), suggesting their importance in maintaining global chromosome architecture.

Eukaryotic chromosomes are packaged into two general types of chromatin that can determine the behavior of the underlying DNA sequence. While euchromatin is typically gene-rich open chromatin, heterochromatin maintained in a condensed state contains primarily repetitive sequences and relatively few genes. Distinct patterns of histone modifications decorate euchromatic and heterochromatic domains. For example, histone H3 methylated at lysine 9 (H3K9me) is preferentially enriched at heterochromatic loci, whereas histone H3 methylated at lysine 4 (H3K4me) marks euchromatic domains (Litt et al., 2001; Noma et al., 2001). Moreover, histones are hyperacetylated at active euchromatic sites but hypoacetylated at heterochromatic loci (Grunstein, 1998). A key feature of heterochromatic complexes is their ability to spread *in cis*, causing epigenetic silencing of adjacent loci (Grewal and Moazed, 2003). However, the encroachment of heterochromatin into euchromatin is prohibited by the presence of boundary elements (Sun and Elgin, 1999; Donze and Kamakaka, 2001; Noma et al., 2001). It has been suggested that these elements could confer boundary function by partitioning autonomous chromosomal domains into "higher-order" loops either by interacting with each other or with some other fixed nuclear structures (Gerasimova et al., 2000; Ishii et al., 2002; Blanton et al., 2003; Yusufzai et al., 2004). In some cases, barrier elements recruit active chromatin-modifying activities, which counteract the propagation of heterochromatin (Litt et al., 2001; West et al., 2004). In budding yeast, the *tRNA* gene located near the silent mating-type locus blocks the

spread of heterochromatin (Donze and Kamakaka, 2001). This *tRNA* gene utilizes RNA polymerase III complex and chromatin-modifying factors to prevent the spread of heterochromatin (Oki and Kamakaka, 2005), but the exact mechanism remains unknown.

The fission yeast *Schizosaccharomyces pombe* genome contains large blocks of heterochromatin at centromeres and subtelomeric regions of all three chromosomes, at tandem *rDNA* arrays and a 20-kilobase silent mating-type (*mat*) interval (Cam et al., 2005). The assembly of a heterochromatic domain has been investigated in detail at the *mat* locus, at which the RNAi machinery and DNA binding factors independently recruit heterochromatic factors such as H3K9me and Swi6/HP1 to specific sites (Hall et al., 2002; Jia et al., 2004; Yamada et al., 2005). Heterochromatin subsequently spreads to the entire silent mating-type interval and is confined to this region by two inverted repeats, *IR-L* and *IR-R*, which surround the heterochromatic domain (Noma et al., 2001; Thon et al., 2002). Consequently, an abrupt transition of euchromatic (H3K4me) and heterochromatic (H3K9me) modifications is observed at sites coinciding with the location of *IR* elements (Noma et al., 2001). Similarly, marked decreases in H3K9me and Swi6 proteins are observed at the borders of pericentromeric heterochromatic domains which are often demarcated by clusters of *tRNA* genes (Partridge et al., 2000; Wood et al., 2002; Cam et al., 2005). However, no *tRNA* gene flanks the right side of centromere 1 (*cen1*) while the left side of *cen1* contains only a single *tRNA* gene, indicating that elements other than *tRNA* genes might be required to contain the spread of heterochromatin outside centromere boundaries. Mapping of heterochromatin and RNAi factors has recently uncovered two inverted repeat elements flanking the left and right sides of *cen1* (*IRC1-L/R*) and *cen3* (*IRC3-L/R*) whose presence coincides precisely with the sharp decreases in heterochromatin and RNAi complexes (Cam et al., 2005). Whether these *IRC* elements indeed possess boundary activity has not been explored. Moreover, it is still unclear how the *IR* elements could function as boundaries at the *mat* locus.

In this study, we utilize an integrated approach, combining genetic and genomic analyses, to gain insights into boundary elements at different sites across the fission yeast genome and also investigate the mechanism of the *IR* boundary function at the *mat* locus. Our analyses suggest that *IRC* elements surrounding centromeres serve as heterochromatin barriers, utilizing a mechanism that is distinct from the *IR* boundaries. The *IR* elements contain multiple *B-box* sequences, well known binding sites for the transcription factor TFIIIC required for Pol III transcription complex assembly, that are critical for boundary activity. These *B-boxes* recruit TFIIIC complex, but not Pol III, to the *IR* elements and are also required for efficient transcription of *IRs* by RNA Pol II. Extending this result to a genome-wide profiling analysis, we unexpectedly identified a number of sites dispersed across the fission yeast genome that are occupied by high concentrations of TFIIIC but not Pol III. We demonstrate that these TFIIIC-bound sequences are tethered to the nuclear periphery in *B-box*-dependent manner. Therefore, our analyses of the *IR* boundaries may have identified a general mechanism for genome organization in fission yeast and other systems.

RESULTS

TFIIIC Localizes at the *IR* Elements of the Mating-Type Locus to Confer Boundary Activity

It has been shown recently that the boundary element at the chicken β-globin locus is highly enriched for active chromatin modifications such as histone acetylation and methylation of H3K4 (Litt et al., 2001), which are recruited by the sequence-specific DNA binding factor USF (West et al., 2004). These histone modifications are believed to counter the spread of repressive heterochromatic complexes. To test whether the *IR* elements at the *mat* locus are similarly enriched for active chromatin modifications, we performed high-resolution chromatin immunoprecipitation (ChIP) analysis, (Noma et al., 2001) comparing the distribution of the euchromatin- and heterochromatin-specific histone modifications around the *IR* elements. We found that the euchromatic histone modifications, H3K9ac, H3K14ac, and H3K4me, were not enriched within the *IR*s, but instead the increased levels of these modifications correlate tightly with euchromatic gene-containing regions outside of the *IR* elements (Figure 1). In contrast to H3K4me, we found that H3K9me was highly enriched at the *IR* elements. The level of H3K9me decreased sharply at a specific site inside the *IR* repeats, which suggests that the actual boundary activity is associated with certain specific sequences within the *IR* elements. To explore the possibility that decreased H3K9me levels might reflect the absence of nucleosomes at these border regions, we mapped the occupancy of histone H3 around the *IR* elements. ChIP analysis revealed no apparent change in nucleosome density around the *IR* repeats (Figures 1B and 1C).

To identify the core sequence responsible for conferring boundary activity to *IR* repeats, we performed heterochromatin-spreading assay using fission yeast strains that carried a series of small deletions within the *IR-R* element. These strains contain *ura4*$^+$ reporter gene inserted on the euchromatic side of the *IR-R*. Loss of *IR-R* resulted in spreading of heterochromatin, causing silencing of the reporter gene (Figure 2A; Noma et al., 2001). Whereas most small deletions did not affect the boundary function of the *IR-R*, a 500 bp deletion near the *IR-R* border toward the euchromatic domain resulted in heterochromatin spreading to the same extent as a complete loss of *IR-R* (Figure 2A). Notably, this 500 bp deleted sequence overlapped with a region in which there was a sharp decrease in H3K9me levels (Figures 1B and 1C).

Sequence analysis of the 500 bp region that is critical for the boundary function of *IR-R* revealed the presence of five *B-box* sequences (Figure 2B). The *B-box* is a high-affinity binding site for TFIIIC that contributes to the promoter activity of *tRNA* genes and other small RNA genes

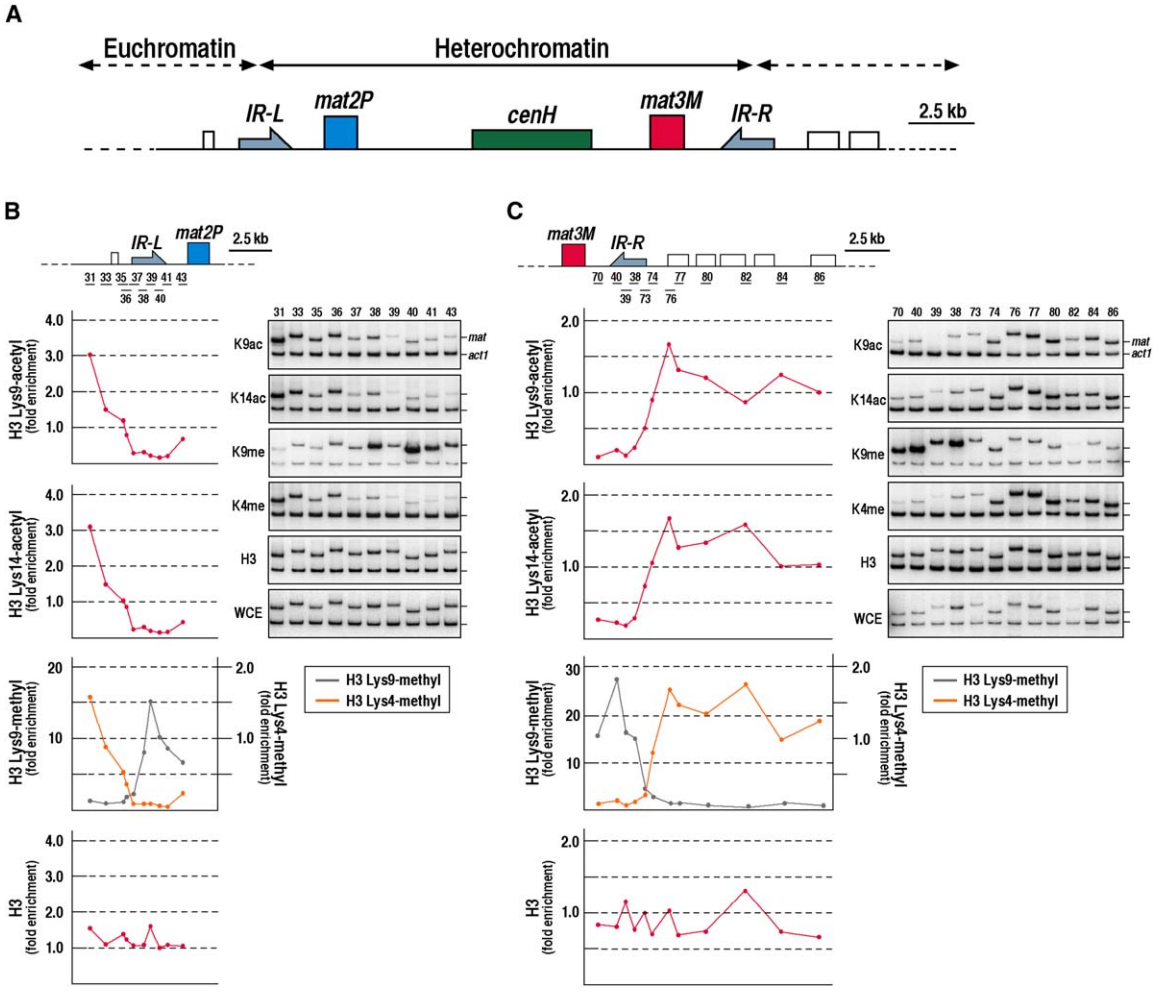

Figure 1. Histone Modifications around the *IR-L* and *IR-R* Boundary Elements

(A) A physical map of the mating-type region. The *IR-L* and *IR-R* inverted repeats surrounding the *mat2/3* heterochromatic domain are shown as light blue arrows. The green box represents the *cenH* sequence that shares homology to centromeric repeats. Open boxes correspond to ORFs.

(B and C) ChIP analysis showing the distribution of histone H3 and its modifications at *IR-L* and *IR-R* using antibodies against histone H3, H3 Lys9-acetyl (K9ac), H3 Lys14-acetyl (K14ac), H3K9-dimethyl (K9me), and H3K4-dimethyl (K4me). DNA isolated from ChIP and WCE fractions was subjected to multiplex PCR to amplify DNA fragments from the mating-type region (*mat*) and an *act1* fragment serving as an amplification control. Numbered bars below the map indicate the primer pairs used in each PCR (Noma et al., 2001). The ratios of the *mat* and control *act1* signals were used to calculate relative fold enrichment values plotted in alignment with the map of the *IR* elements.

transcribed by Pol III. TFIIIC is a highly conserved multisubunit complex consisting of two interconnected lobular domains, one of which is composed of Sfc3 and Sfc6 proteins (Huang and Maraia, 2001). To assess whether the *B-boxes* within the *IR* element have a role in boundary activity, we constructed a strain carrying a *B-box* deletion at the *IR-R* (*B-box⊿*). Deletion of the *B-boxes* resulted in heterochromatin spreading (Figure 2A), concomitant with increased H3K9me and decreased H3K4me levels outside of the *IR-R* (Figure 2C). We next investigated whether components of TFIIIC are localized at the *IR* elements. ChIP analysis revealed that Sfc6 was localized at the *IR-R* region containing the *B-boxes* (Figure 2D), while deletion of *B-boxes* completely abolished Sfc6 enrichment (Figure 2E). Furthermore, insertion of three tandem copies of synthetic *B-boxes* in *IR-R⊿* strain could restore TFIIIC binding and heterochromatin boundary (Figures 2F and 2G). From these analyses, we conclude that *B-box* sequences within the *IR* elements surrounding the silent *mat* region recruit TFIIIC components and are responsible for the boundary activity associated with these inverted repeats.

B-boxes Are Required for Pol III-Independent Transcription of *IR* Elements

The presence of *B-boxes* and the localization of TFIIIC at the *IR* elements prompted us to examine whether the *IR*s are transcribed. We detected at least two distinct

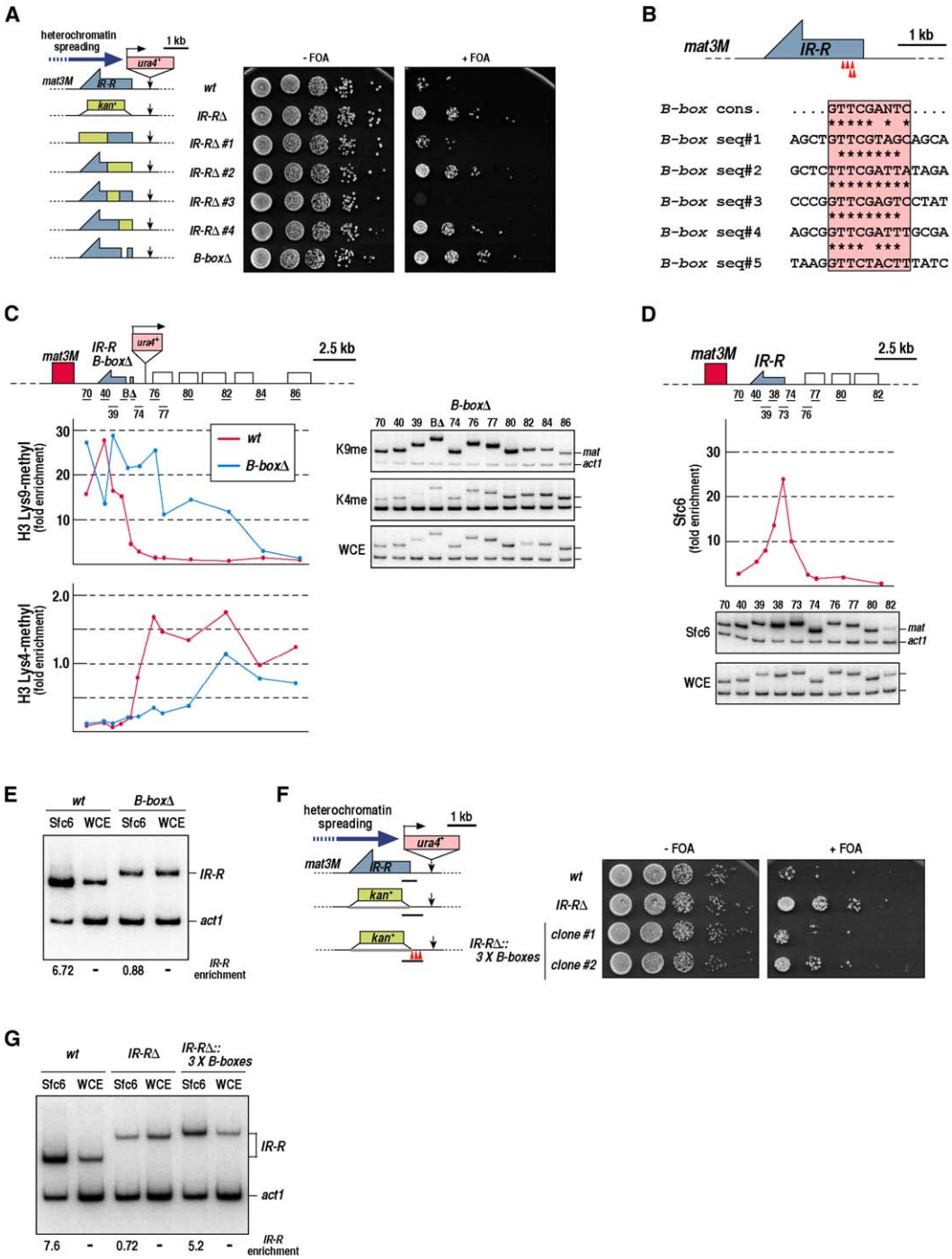

Figure 2. TFIIIC Binding at the *IR-R* Element Is Required for Boundary Activity

(A) Identification of boundary core sequence. Different portions of the *IR-R* were replaced with *kan*$^+$ gene (green boxes; not drawn to scale). The *B-box⊿* cells lack a 240-bp sequence that contains 5 *B-boxes* and do not carry the *kan*$^+$ gene. Serial dilution plating assays in the presence and absence of FOA were done to measure the expression of *ura4*$^+$ marker inserted just to the right of the *IR-R*. Growth on FOA plate indicates repression of the *ura4*$^+$ gene.

(B) *B-boxes* at the *IR* element. Red arrows indicate the positions of the *B-boxes*. The *B-box* sequences from the *IR* are aligned with the *B-box* consensus sequence present at *tRNA* genes (Hamada et al., 2001). Asterisks indicate conserved nucleotides.

(C) Heterochromatin spreading beyond the *IR* lacking *B-boxes*. H3K9me and H3K4me levels as determined by ChIP are shown.

(D) Localization of the TFIIIC component, Sfc6, at the *IR*. Levels of Sfc6 binding at *IR-R* were determined by ChIP.

(E) *B-boxes* are required for Sfc6 binding at *IR*. Sfc6 levels at *IR-R* in wild-type (*wt*) or *B-box*-deficient strains (*B-box⊿*) were measured by ChIP. Multiplex PCR was performed using primers that specifically amplify the *IR-R* element (primer pairs 73 for wild-type [Figure 2D] and BΔ for

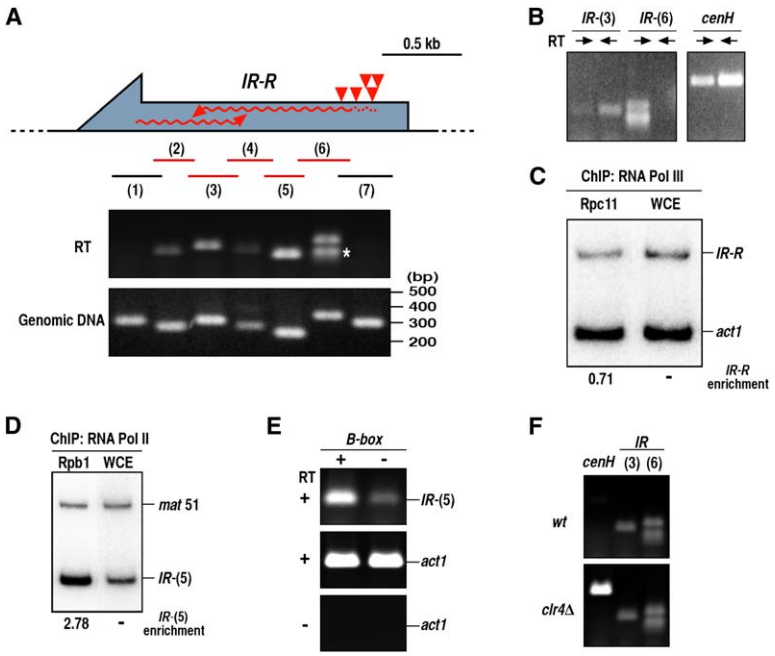

Figure 3. Analysis of Transcripts Generated from the *IR* Element

(A) Detection of transcripts from the *IR*. RT-PCR was performed using primer pairs 1–7. Arrowheads indicate *B-box* positions. Red wavy lines represent predicted transcripts based on results shown in Figures 3A and 3B. The asterisk indicates spliced transcript derived from the *IR*, as confirmed by DNA sequencing. PCR with genomic DNA as template is shown as a control (bottom). RT, reverse transcription.

(B) Direction of *IR* transcription. Strand-specific RT-PCR was performed as described previously (Noma et al., 2004). Arrows indicate the direction of the primer used in first strand cDNA synthesis. The *cenH* primer pair was used as a positive control as both strands of *cenH* are known to be transcribed.

(C) RNA Pol III subunit, Rpc11, does not localize to the *IR-R*, as determined by ChIP.

(D) Localization of the RNA Pol II subunit, Rpb1, at the *IR*. Level of Rpb1 at the *IR-R* was determined by ChIP using the *IR*-(5) and *mat* 51 primer pairs. The *mat* 51 primer pair amplifies a sequence located at the silent mating-type region that is not transcribed even in the absence of heterochromatin.

(E) Deletion of the *B-box* region results in reduced transcription at the *IR*. Transcript levels were analyzed by RT-PCR using RNA samples prepared from strains with (+) or without (−) the *B-boxes* at the *IR-R*. Experiments were performed using *IR-LΔ swi6*⁻ strains.

(F) Heterochromatin-independent transcription of the *IR*. The *IR* and *cenH* transcripts were analyzed by RT-PCR with RNA samples purified from wild-type (*wt*) or *clr4Δ* cells.

transcripts produced from the *IR*s by RT-PCR assay (Figure 3A). One of these transcripts is initiated near the tail end of the *IR*s, where TFIIIC is bound to *B-boxes*. However, the second transcript, which occurred in the opposite direction (designated as the reverse transcript), is initiated from a different region near the tip of the *IR* elements (Figure 3B). Transcripts originating from both strands of the *IRs* could be detected in the middle portion of the *IR* element (Figure 3B, primer pair 3). RT-PCR analysis also suggested that the forward transcript might be processed as indicated by two different size RNA species (Figure 3A, primer pair 6). Indeed, sequencing showed that the shorter transcript results from splicing of an intron, which contains canonical splicing donor and acceptor motifs found in Pol II transcribed genes (data not shown; Kuhn and Kaufer, 2003).

TFIIIC recruitment to the *B-boxes* at the *IR*s suggested that Pol III might transcribe these elements. Surprisingly, we did not detect Pol III binding at the *IR* elements whereas Pol III was detected at *tRNA* genes (Figure 3C; see below). Furthermore, the *IRs* contain internal stretches of ≥5 T residues, termination site hallmark of Pol III, suggesting that Pol III is unlikely responsible for *IR* transcription. However, we could detect the binding of Pol II subunit, Rpb1, at the *IR*s (Figure 3D), indicating that despite the presence of TFIIIC at the *IR* boundaries, Pol II might direct transcription of these elements. To determine the effect of TFIIIC binding on *IR* transcription, levels of *IR* transcripts were analyzed in wild-type and *B-boxΔ* cells (Figure 3E). Since *IR* elements are identical in sequence, we performed this experiment using a strain that carries deletion of *IR-L* to specifically assay transcripts derived only from the *IR-R* element carrying *B-box* deletion. Although low levels of forward transcripts could still be detected in *B-boxΔ* cells, they were drastically reduced compared to wild-type cells (Figure 3E), suggesting that TFIIIC bound to *B-boxes* could modulate Pol II transcriptional activity at the *IRs*. However, we cannot exclude the possibility that the deleted region occupied by the *B-boxes* might also contain promoter element important for Pol II transcription.

Bidirectionally overlapped transcription in the middle portion of the *IR*s suggested that transcripts produced from these elements might be subjected to RNAi-mediated

B-boxΔ strain [Figure 2C]) and *act1* primers. Intensities of bands representing *IR* and *act1* in ChIP and WCE lanes were used to calculate relative enrichment shown below ChIP lane.

(F and G) Synthetic *B-boxes* confer boundary activity. Strain carrying *IR-RΔ::3 X B-boxes* was created similar to IR-Rs strain but containing three tandem copies of 11 nucleotides *B-box* consensus sequence (red triangles). Black bold line below each map indicates the PCR fragment used for ChIP analysis shown in Figure 2G.

heterochromatic silencing. However, deletion of *clr4*, which abolishes heterochromatin and results in enhanced *cenH* transcripts (Noma et al., 2004), did not affect *IR* transcript levels (Figure 3F), suggesting that transcription at the *IR*s is not subjected to heterochromatin-mediated control.

TFIIIC and Pol III Factors Are Enriched at Centromere Heterochromatin Boundaries

To investigate whether TFIIIC might have a more extensive role in boundary function at other chromosomal regions, we performed genome-wide mapping of Sfc6, a subunit of TFIIIC. In addition, we also probed the distribution of Pol III by mapping its subunit, Rpc130. Although TFIIIC and Pol III complexes are known to control transcription of *tRNA* and *5S rRNA* genes (Weinmann and Roeder, 1974; Paule and White, 2000), systematic mappings of both Pol III and TFIIIC complexes across the fission yeast genome have not been performed. Our analyses revealed that both TFIIIC and Pol III were enriched at the promoters of *tRNA* and *5S rRNA* genes (Figure 4). Surprisingly, we also observed high concentrations of TFIIIC in the absence of Pol III at many sites dispersed across the genome (below). There was, on average, more than 14-fold enrichment for Pol III and more than 6-fold enrichment for TFIIIC at all *tRNA* genes (Figure S1), in agreement with observations in budding yeast (Roberts et al., 2003; Moqtaderi and Struhl, 2004). Similarly, Pol III was also highly enriched at all *5S rRNA* genes (>12 fold), while TFIIIC was only modestly enriched at these gene loci (Figure S1).

Previous genome-wide analysis of heterochromatin distribution in fission yeast genome has suggested the potential existence of boundaries surrounding the major heterochromatic domains (Cam et al., 2005). To determine whether binding of TFIIIC was associated with barriers that partition heterochromatin from euchromatin, genome-wide maps of Sfc6 and Rpc130 were overlaid with previous maps of H3K4me and H3K9me. In agreement with conventional ChIP analysis (Figure 2), ChIP-chip results revealed two prominent peaks of TFIIIC enrichment at the *IR* elements flanking the heterochromatin domain of the silent *mat* interval (Figure 4B). Strikingly, the high concentrations of TFIIIC at the *IR*s occurred in the absence of Pol III. Our mapping revealed little or no enrichment of TFIIIC nor Pol III at the subtelomeric regions and tandem *rDNA* array that are also coated with heterochromatin complexes (Figures 4C and S2), suggesting that alternative mechanisms might be involved in blocking the spread of heterochromatin at these loci. However, we found high enrichment for both TFIIIC and Pol III complexes at the boundaries of heterochromatin domains associated with pericentromeric repeats, which contain clusters of *tRNA* genes (Figure 4D). Akin to the *IR* elements, the high enrichment of TFIIIC at these *tRNA* gene clusters may be sufficient to counter the spread of pericentromeric heterochromatin. Interestingly, at *cen1*, only a single *tRNA* gene flanks the left side of its heterochromatin domain while there is no *tRNA* gene flanking its right side (Figure 4D). Moreover, despite a high enrichment for Pol III at this single *tRNA* gene, TFIIIC was only modestly enriched, indicating that this single *tRNA* gene may possess only weak boundary activity and that it may need the cooperation from other nearby *cis*-elements to prevent heterochromatin spreading. Indeed, we have shown previously that two inverted repeat (*IRC*) elements flank *cen1* and *cen3*, which might possess boundary activities (Cam et al., 2005).

IRC1 Element Functions as Centromere Heterochromatin Boundary

To help uncover sequences critical for boundary function at *cen1*, we performed high-resolution mapping of heterochromatin- and euchromatin-specific histone modifications. As indicated by a sharp decrease in H3K9me level at site corresponding to the *IRC1-L*, the boundary between pericentromeric heterochromatin and surrounding euchromatic domains seems to coincide with the location of the *IRC1* element (Figures 5A and 5B). The marked decrease in H3K9me levels was not due to lower H3 occupancy because active chromatin modifications such as H3K4me, H3K9ac, and H3K14ac were highly enriched at the *IRC1* and its flanking sequences (Figure 5B), consistent with our earlier work showing that *IRC* elements are actively transcribed by Pol II (Cam et al., 2005). To directly test whether *IRC1* and $tRNA^{phe}$ gene are required for the boundary function, we constructed strains containing small deletions encompassing $tRNA^{phe}$ gene, *IRC1-L,* or intervening sequences. We studied the effects of these deletions on silencing of $ura4^+$ reporter gene inserted at a region immediately centromere-distal to the $tRNA^{phe}$ gene to assay for the spread of heterochromatin. While deletion of $tRNA^{phe}$ gene (*cen1LΔ#1*) or surrounding sequences (*cen1LΔ#2*) had no measurable effect on silencing of the reporter gene, *IRC1Δ* (*cen1LΔ#3*) led to a significant increase in fraction of cells in which $ura4^+$ is silenced (Figure 5C). This increase in silencing of the reporter gene in *IRC1Δ* (*cen1LΔ#3*) cells correlated with the spreading of H3K9me and concomitant decrease in H3K4me levels at adjoining euchromatic region (Figures 5C and 5D). These analyses suggest that *IRC1* is the predominant boundary at *cen1,* preventing the spread of pericentromeric heterochromatin beyond its natural boundary.

We next explored whether *IRC1* boundary might also employ TFIIIC-based mechanism similar to the *IR* elements. Conventional ChIP analysis showed that Sfc6 was enriched at the $tRNA^{phe}$ gene, as expected, but the levels of Sfc6 were significantly lower than observed at the *IR*s (Figure 5B). However, we did not detect TFIIIC binding at the *IRC1* (Figure 5B), suggesting that these inverted repeat elements likely utilize a distinct boundary mechanism(s). This result is also consistent with our ChIP-chip analysis showing that TFIIIC and Pol III are not localized at the boundary on the right side of *cen1* where *IRC1* alone marks the heterochromatin/euchromatin border (Figure 4D).

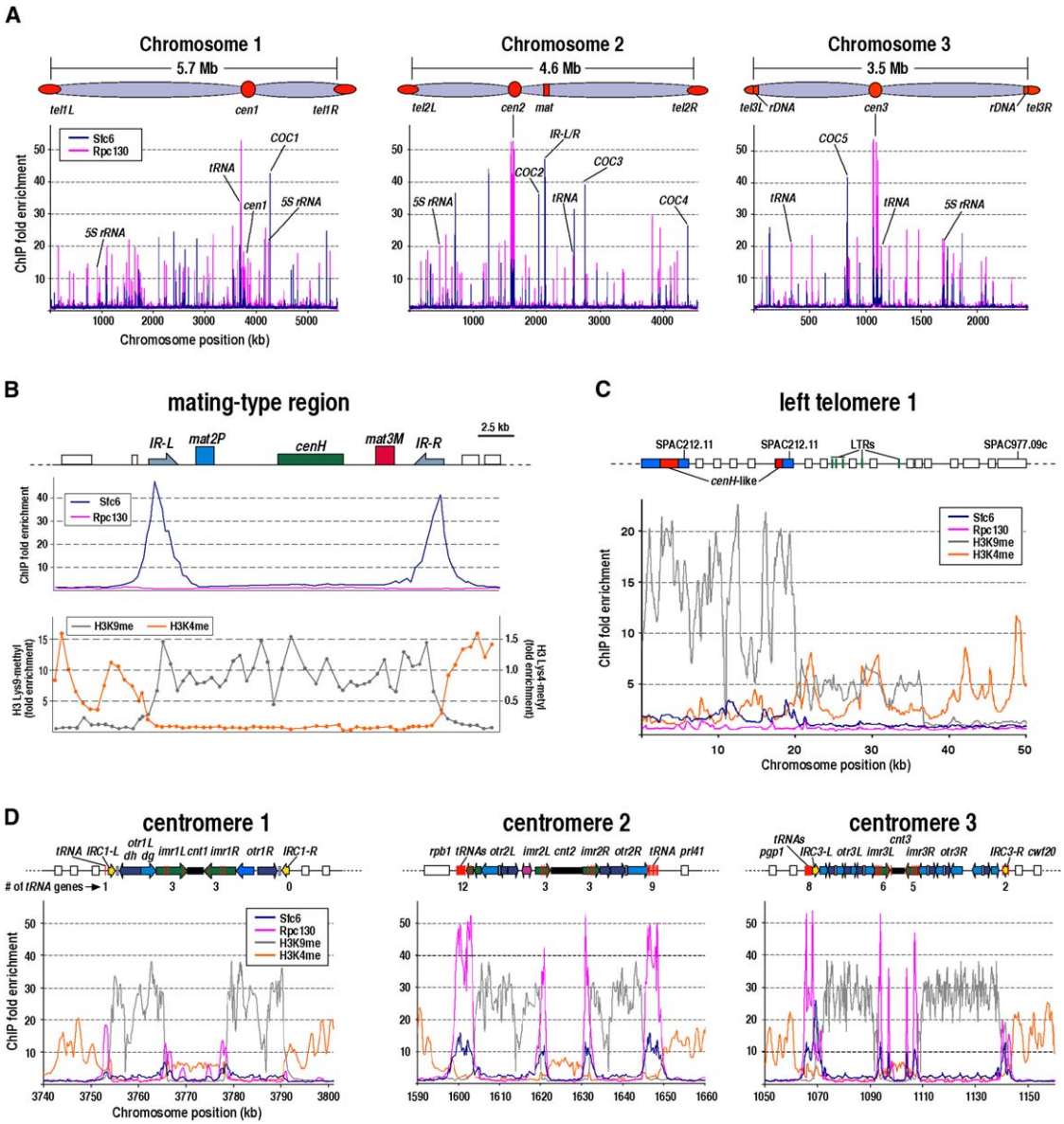

Figure 4. Genomewide Distributions of TFIIIC (Sfc6) and Pol III (Rpc130)

(A) Chromosomal distribution profiles of Sfc6 and Rpc130. Schematic diagrams of *S. pombe* chromosomes are shown (top). Relative enrichments of Sfc6 and Rpc130 are plotted with respect to chromosome position. The centromere regions (*cen1-cen3*), the *IR-R/L* at the mating-type region, and TFIIIC-associated *COC* loci (see text) are indicated together with selective peaks corresponding to *tRNA* and *5S rRNA* genes.

(B) Distributions of Sfc6, Rpc130, H3K9me, and H3K4me at the mating-type region. The distributions of H3K9me and H3K4me were derived from high-resolution mapping by conventional ChIP analysis (Noma et al., 2001).

(C) Distributions of Sfc6, Rpc130, H3K9me, and H3K4me at the subtelomere on the left arm of the chromosome 1. Green vertical lines and white boxes denote retrotransposon long terminal repeats (LTRs) and ORFs, respectively. SPAC212.11 (blue boxes), a *recQ* helicase, contains *cenH*-like sequence (red boxes). H3K9me and H3K4me distributions were described previously (Cam et al., 2005).

(D) Distributions of Sfc6, Rpc130, H3K9me, and H3K4me at centromeres. Physical maps of *S. pombe* centromeres denoting centromeric *otr* regions comprised of *dg* and *dh* elements, *imr* and *cnt,* are shown (top), with the number of *tRNA* genes within each region shown directly below. Red vertical lines (*tRNA* genes); open boxes (ORFs); Inverted repeat elements flanking *cen1* (*IRC1-L/R*) and *cen3* (*IRC3-L/R*) (yellow arrows).

TFIIIC Localizes to Divergent Pol II Gene Promoter Regions without Recruiting Pol III

While TFIIIC and Pol III were found at all *tRNA* gene loci, genome-wide analysis revealed that, similar to the *IR* elements, TFIIIC was found at high concentrations at many distinct sites across the genome that showed little or no enrichment for Pol III (Figure 4A). We refer to these sites as *COC* loci (see below), and loci most highly enriched

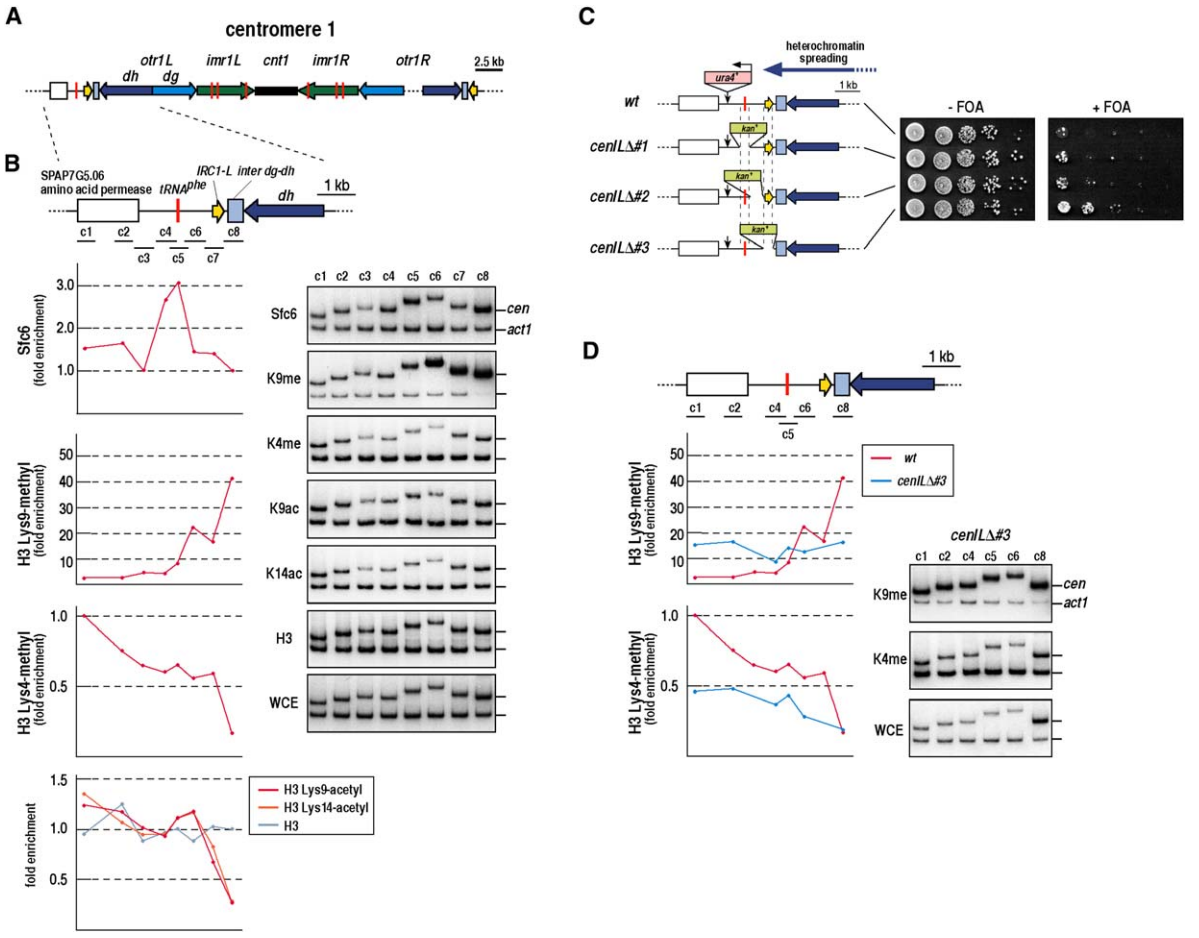

Figure 5. *IRC1* Acts as Heterochromatin Boundary

(A) Physical map of centromere 1. *cen1* consists of the *cnt1*, *imr1* repeats (*imr1L* and *imr1R*) and *otr1* repeats (*otr1L* and *otr1R*). *tRNA* genes (red vertical lines); inverted repeat elements flanking *cen1* (*IRC1-L/R*) (yellow arrows).

(B) Mapping of TFIIIC (Sfc6) and histone modifications at *IRC1-L*. Schematic map of *IRC1-L* is shown (top panel). Numbered bars (c1–c8) below the map indicate primer pairs used in ChIP.

(C) Identification of boundary sequence at the *IRC1-L*. A series of sequence deletion replaced with *kan*$^{+}$ marker gene (light green boxes) was made at *IRC1-L* and adjoining regions. Serial dilution plating assays in the presence and absence of FOA were performed to measure expression of *ura4*$^{+}$ marker inserted at the centromere-distal side of the *tRNA*^{phe} gene.

(D) Heterochromatin spreading in *IRC1-L∆* cells. Levels of H3K9me and H3K4me in wild-type (*wt*) and *cen1L∆#3* strains determined by ChIP are shown in alignment with the map of *IRC1-L* region.

for TFIIIC are indicated (Figure 4A and Table S1). Conventional ChIP assay confirmed that TFIIIC subunits Sfc1, Sfc3, and Sfc6 localized to these loci while Rpc11 and Rpc130 subunits of Pol III were absent (Figure 6A). To further explore the significance of these TFIIIC-associated sites, we examined the top 23 sites with greater than 10-fold enrichment for Sfc6 (Table S1). We found that for 91% of these sites, the peaks of TFIIIC enrichment were located within a few hundred bases upstream of the coding region that overlaps with gene promoters (Figure 6B). Similar to the *IR* boundaries, multiple *B-boxes* are located at these TFIIIC peaks (Figure 6B). Intriguingly, most of these gene promoters are divergent, and previous gene-expression profiling indicates that the regulation of those nearly genes is generally independent of the cell cycle (Rustici et al., 2004). These data point to an unanticipated role for TFIIIC in modulating the expression of Pol II genes and suggest that high concentrations of TFIIIC localize to previously unknown sites in the genome that, unlike *tRNA* genes, are characterized by a lack of Pol III.

Immunofluorescent Localization of TFIIIC and Its Associated Loci Uncovers a Possible Role for TFIIIC in Nuclear Organization

We next sought to understand the mode of action of TFIIIC in boundary function. We hypothesized previously that factors bound to the *IR* boundaries surrounding the silent *mat* locus might facilitate tethering of these sequences to subnuclear structures (Noma et al., 2001), similar to proposed mechanisms in other systems (Gerasimova et al.,

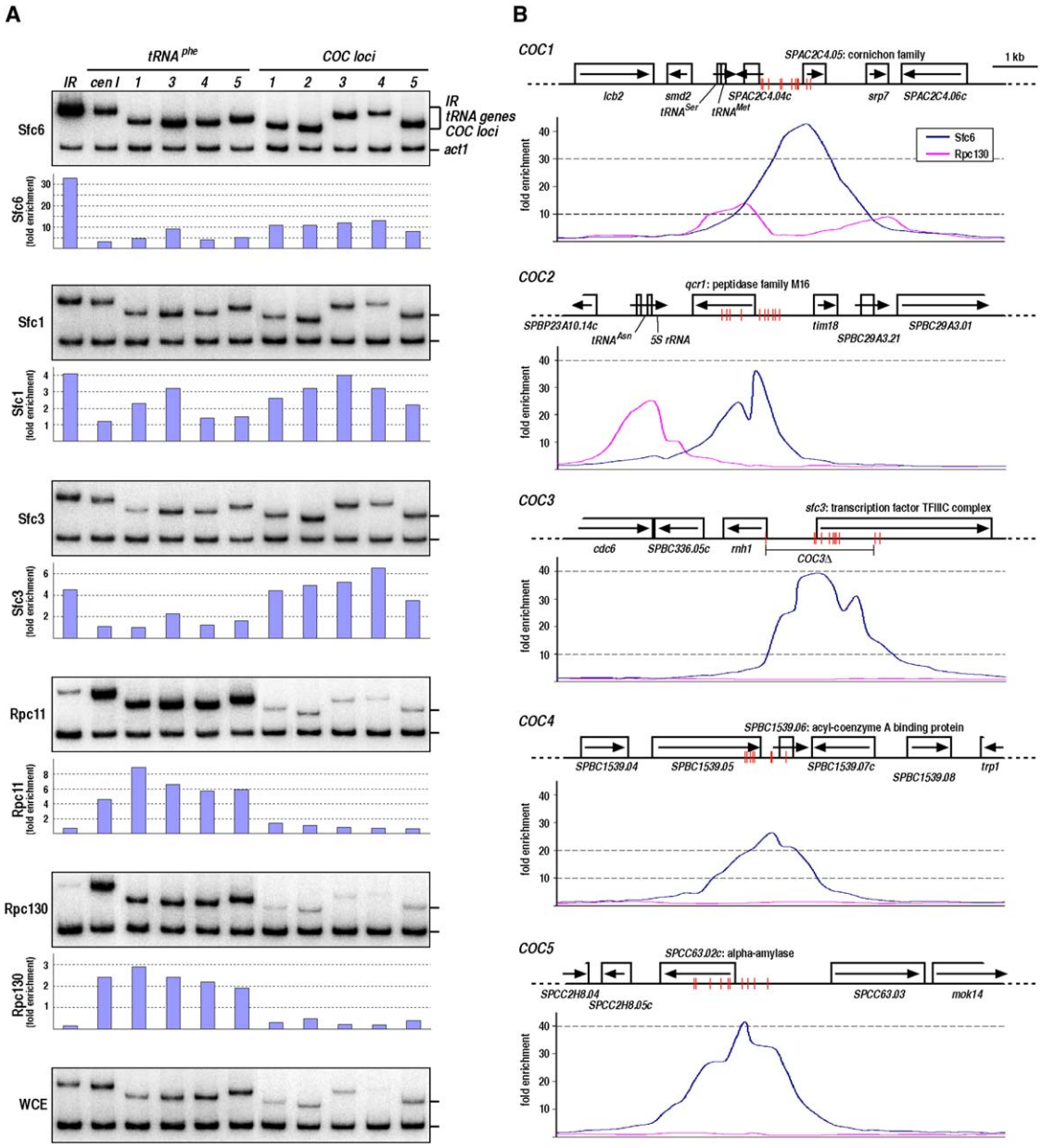

Figure 6. TFIIIC Associates with Multiple *COC* Loci Independent of Pol III

(A) TFIIIC, but not Pol III, associates with *COC* loci. Localizations of TFIIIC components (Sfc6, Sfc1, and Sfc3) and Pol III components (Rpc11 and Rpc130) at the *IR*, *tRNA* genes, and *COC* loci were analyzed by conventional ChIP assays. ChIP and WCE signals were used to calculate enrichment of TFIIIC and Pol III.

(B) Distributions of the Sfc6 and Rpc130 at and around the *COC* loci as determined by ChIP-chip analyses. ORFs (open boxes); putative *B-boxes* (red vertical lines). Annotations of genes containing Sfc6 binding peaks within their promoter regions are shown. Note that while *COC* loci are associated only with Sfc6, both Sfc6 and Rpc130 are localized at *tRNA*s, *5S rRNA,* and *srp7* (7SL signal recognition particle component), which reside near *COC1* and *COC2* loci.

2000; Ishii et al., 2002; Yusufzai et al., 2004). We directly tested this possibility by determining the localization of TFIIIC within the nucleus by immunofluorescent staining of Sfc3 and Sfc6 proteins. Remarkably, Sfc3 and Sfc6 were most highly concentrated at five to ten bodies present at the nuclear periphery with a subset of these bodies located in proximity to the nucleolus (Figures 7A and S3). To determine whether TFIIIC-associated loci also associate with the nuclear periphery, we performed fluorescent in situ hybridization (FISH) analysis using probes specific to the randomly selected high affinity TFIIIC binding sites. Consistent with TFIIIC bodies located at the nuclear

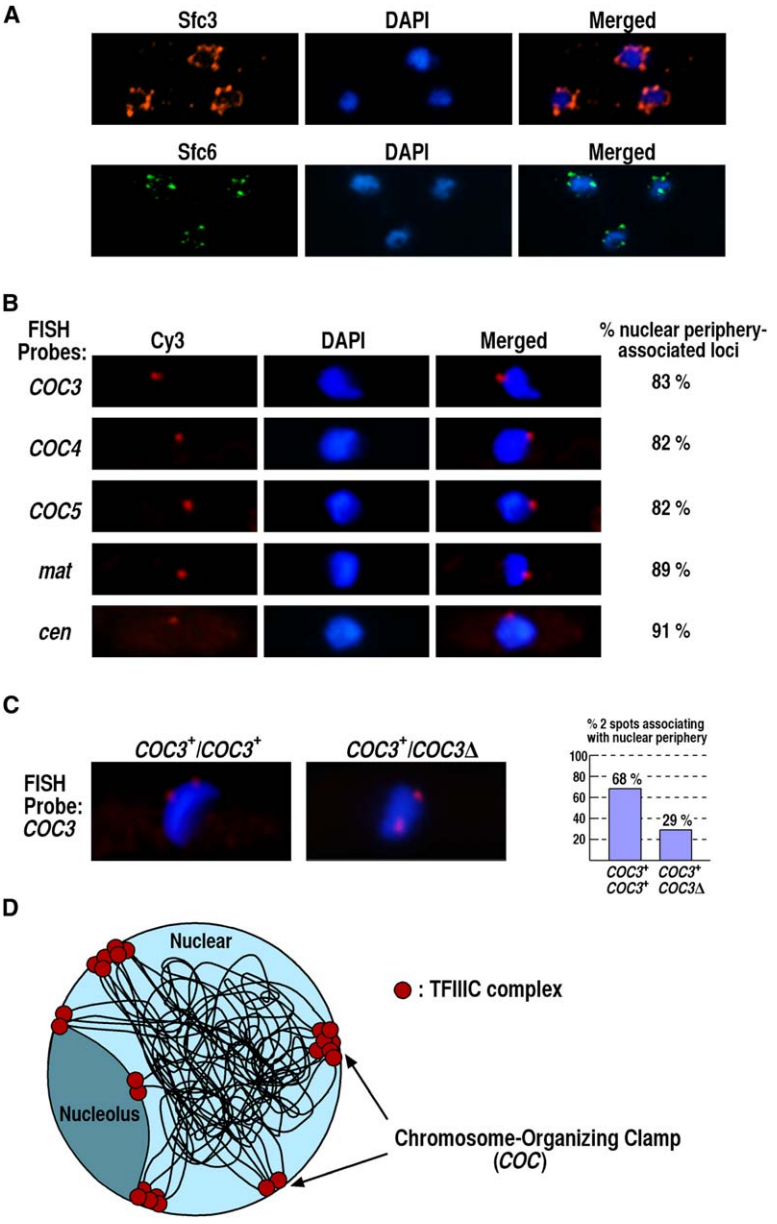

Figure 7. A Role for TFIIIC in Genome Organization

(A) TFIIIC bodies at the nuclear periphery. Deconvoluted immunofluorescent images of cells stained for either Flag-Sfc3 (red) or Sfc6-Myc (green) proteins were merged with DAPI signals (blue).

(B) FISH analysis of *COC* loci in fission yeast nucleus. *COC3*, *COC4*, *COC5*, the mating-type region, and centromeres were visualized by FISH using Cy3-conjugated probes (red). FISH signals that lie at the edge of the DAPI signal were counted as loci associated with the nuclear periphery. More than 200 cells were counted for each probe.

(C) Effect of *COC3Δ* on the localization of *COC3* site within the nuclei of diploid cells. Deleted *COC3* sequence is indicated in Figure 6B. Only cells displaying two discrete FISH signals as well as DAPI signal were investigated by microscopy. More than 100 cells were analyzed, and the results are summarized in graph (right panel).

(D) A model for the role of TFIIIC in genome organization. The recruitment of TFIIIC to *IRs* and *COC* loci facilitates tethering these loci to the nuclear periphery. TFIIIC signal was also detected around the surface of the nucleolus. This nuclear peripheral tethering might restrict the spread of heterochromatin to surrounding sequences. TFIIIC localization at centromeric *tRNA* gene clusters could also contribute to barrier activity associated with these regions. TFIIIC localized at *COC* loci might facilitate the clustering of distant chromosomal loci into a few distinct nuclear bodies, thus creating a higher-order chromosome organization that imparts different properties on these regions including transcriptional regulation of nearby genes.

periphery, TFIIIC-associated sites including the *mat* locus, centromeres and several *COC* loci were also found to be predominantly associated with the nuclear periphery (Figure 7B). The association of TFIIIC loci with the nuclear periphery led us to hypothesize that these loci might have a role in organizing the fission yeast genome. Specifically, TFIIIC-occupied sites dispersed across the genome, including the divergent promoters, might act as Chromosome-Organizing Clamps (*COC*) to tether these chromosomal regions to the nuclear periphery. Indeed, we found that *COC1* could partially substitute the *IR-R* element at the *mat* region as heterochromatin barrier (Figure S4). Since our analyses showed high concentrations of TFIIIC at more than 60 distinct sites, but only five to ten TFIIIC bodies could be visualized at the nuclear envelope, it is likely that TFIIIC-associated loci cluster together to a few common regions at the nuclear periphery. Such clustering of sequences at TFIIIC bodies might result in the high concentrations of TFIIIC observed at the *COC* sites and at the boundary elements (Figure 6B).

B-box Sequences Are Essential for Tethering *COC* Sequences to the Nuclear Periphery

To examine whether TFIIIC binding is essential for tethering *COCs* to the nuclear periphery, we constructed a diploid strain in which one of the two *COC3* alleles was deleted (Figure 6B), and we used this strain to study the effects of *COC3Δ* on the nuclear localization of surrounding sequences. Diploid cells rather than haploid cells were used because many of the *COC* sites including *COC3* are

located adjacent to essential genes. Therefore, deletion of *B-box* sequences is expected to impair the function of these genes, similar to transcriptional defects of *IR* elements lacking *B-boxes* (Figure 3). FISH analysis with a probe corresponding to the sequence surrounding *COC3* site was performed using either *COC3*$^{+}$/*COC3*$^{+}$ or *COC3*$^{+}$/*COC3Δ* diploid cells. Microscopic examination of the cells carrying two discrete spots corresponding to two alleles in a diploid cell showed that in most wild-type *COC3*$^{+}$/*COC3*$^{+}$ cells both spots associated with the nuclear periphery, whereas in a *COC3*$^{+}$/*COC3Δ* diploid cells there was a dramatic reduction in the frequency of both spots simultaneously associating with the nuclear periphery (Figure 7C). In particular, one of the spots in cells carrying *COC3Δ* allele seemed to display random localization pattern. This result suggests that *B-boxes* are essential for tethering *COC* loci to the nuclear periphery.

DISCUSSION

The assembly of heterochromatin domains involves recruitment of silencing complexes to nucleation sites followed by propagation of these complexes in stepwise manner along the chromatin fiber (Grewal and Moazed, 2003). Spreading of heterochromatin beyond its natural borders is blocked by boundary elements. Previous studies have identified boundary elements surrounding heterochromatic domains in fission yeast genome, but the mechanism of boundary function has remained elusive. Our study shows that TFIIIC binds to the *B-box* sequences embedded within boundary elements, which are critical for blocking the spread of heterochromatin to nearby sequences. These TFIIIC binding sites are distinctive in their high concentration of TFIIIC and lack of associated Pol III. Moreover, high levels of TFIIIC are present at many sites scattered across the genome, designated as *COC* loci, which are also devoid of Pol III binding. We demonstrate that TFIIIC is concentrated at five to ten bodies located at the nuclear periphery and that the *B-box* sequences to which TFIIIC binds mediate the tethering of these sites to the nuclear periphery. These interactions may facilitate ''higher-order'' organization of the fission yeast genome into distinct structures, perhaps loops, which likely have implications for diverse chromosomal processes in addition to creating heterochromatin barriers. We also define another class of heterochromatin barrier acting at centromeres that does not utilize TFIIIC mechanism but that is dynamically targeted by the RNAi machinery. Our results indicate that genomes of single cell eukaryotes such as fission yeast might display a specific functional architecture within the nucleus, similar to higher eukaryotes.

Boundaries of Heterochromatin Domains in the Fission Yeast Genome

A remarkable feature of heterochromatic domains associated with fission yeast silent mating-type locus and pericentromeric repeats is a marked decrease in H3K9me and Swi6 observed on both sides of these domains. The transition between domains heavily coated with heterochromatic complexes and surrounding loci is marked by the presence of boundary elements. As described above, the *IR* elements serve as heterochromatin barriers at the *mat* locus (Noma et al., 2001), whereas *tRNA* genes have been suggested to act as barriers at centromeres (Partridge et al., 2000; Cam et al., 2005; Scott et al., 2006). Results described here suggest that *IRs* and *tRNA* genes might share a common boundary mechanism. We discovered that the *IR* elements consist of multiple *B-boxes*, the binding sites for TFIIIC that initiates assembly of *tRNA* Pol III transcription complexes (Weinmann and Roeder, 1974; Paule and White, 2000). TFIIIC binds to the *IR*s in a *B-box*-dependent manner and that *B-boxes* are critical for boundary activity. Moreover, we further showed that synthetic *B-box* consensus sequences, the high specificity TFIIIC binding sites, could act as heterochromatin barrier. Unlike boundaries in *S. cerevisiae*, which require fully assembled RNA Pol III complex to resist the spread of heterochromatin (Donze and Kamakaka, 2001), our analyses suggest that TFIIIC recruitment to the *IR* elements, even in the absence of the other Pol III complex components, is sufficient to establish a functional boundary. The lack of TFIIIC-associated Pol III may reflect a requirement for an upstream TATA box that is critical for the recruitment of TFIIIB and Pol III in fission yeast (Hamada et al., 2001). Therefore, it is conceivable that the boundary activity of TFIIIC could be distinguished from its general role in Pol III transcription. However, TFIIIC mutants that specifically affect boundary activity without affecting Pol III function have not yet been identified. Human TFIIIC component, hTFIII90, contains histone acetyltransferase (HAT) activity (Hsieh et al., 1999). Although we could not detect significant enrichment of histone acetylation at the *IR* elements, it is still possible that low enrichment of histone acetylation could facilitate *IR* boundary activity. Moreover, TFIIIC-associated HAT activity might affect expression of genes located near *COC* sites.

Heterochromatin domains at *cen1* and *cen3* are flanked by inverted repeat elements *IRC1* and *IRC3*, respectively (Cam et al., 2005). We demonstrate that the *IRC1* positioned at the heterochromatin/euchromatin borders might also serve as heterochromatin barriers. The mode of action of the *IRC1* boundaries seems distinct from the *IR* boundaries. In contrast to the high levels of TFIIIC at the *IR* elements, no TFIIIC was detected at the *IRC1*. Instead, *IRC1* transcribed by Pol II (Cam et al., 2005) show significant enrichment of active chromatin modifications such as histone hyperacetylation and H3K4me, that might be essential for counteracting the propagation of heterochromatic structures, as also suggested in other systems (West et al., 2004; Oki and Kamakaka, 2005). Since *tRNA* gene clusters coated with TFIIIC and Pol III flank *IRC* elements in some cases, it is possible that *tRNA* genes cooperate with *IRCs* to efficiently block encroachment of heterochromatin complexes. This situation is analogous to the chicken β-globin and *S. cerevisiae* *HMR* loci, which use multiple mechanisms to prevent the

spread of repressive complexes (Recillas-Targa et al., 2002; Oki and Kamakaka, 2005). A recent study showed that transcripts produced by the *IRC* elements are converted into siRNAs by the RNAi machinery, raising the possibility that siRNAs might have a structural role in creating functional boundaries (Cam et al., 2005). Indeed, production of siRNAs has been shown to be essential for clustering of fission yeast telomeres at the nuclear periphery (Hall et al., 2003; Sugiyama et al., 2005).

ChIP-chip analysis indicated that the TFIIIC-dependent boundaries are not associated with heterochromatin domains at the subtelomeric regions, which display a gradual transition of heterochromatin/euchromatin distribution (Cam et al., 2005). These loci might utilize "negotiable" boundary mechanisms, in which case balance between opposing effects of histone modifying activities or the presence of histone variants such as H2A.Z controls the spread of heterochromatin (Kimura et al., 2002; Suka et al., 2002; Meneghini et al., 2003). Furthermore, specialized factors such as the jmjc domain protein Epe1, which modulates heterochromatin stability by negatively affecting stability of heterochromatic modifications such as H3K9me, are expected to be important in limiting the spread of heterochromatin (Ayoub et al., 2003).

Mechanism of TFIIIC-Mediated Genome Organization and Its Relationship to Other Systems

Studies from different systems have led to distinct models to explain how boundary elements can block the spread of heterochromatic structures. It has been hypothesized that the stable binding of Pol III machinery establishes a nucleosome free region at the *tRNA* gene in *S. cerevisiae* that is sufficient to block the spread of heterochromatin (Bi et al., 2004; Oki and Kamakaka, 2005). Furthermore, Pol III complex and chromatin-modifying activities recruited at the boundary elements have been suggested to create a local chromatin environment less favorable for the spread of heterochromatin (Oki and Kamakaka, 2005). To this end, the binding of TFIIIC to boundary elements per se might be sufficient to prevent heterochromatin spreading. Our analysis also suggests a possible role for boundary elements in nuclear organization. Specifically, we show that TFIIIC localizes to approximately 5–10 bodies at the nuclear periphery and that sites occupied by high concentrations of TFIIIC are tethered to the nuclear periphery, which likely have implications not only for boundary mechanism but perhaps also for genome organization in general (Figure 7D). Apart from the heterochromatic loci, which are presumably tethered to the nuclear periphery via multiple mechanisms, several *COC* sites dispersed across the fission yeast genome are localized at the nuclear periphery. This nuclear-peripheral tethering of a *COC* locus is lost in cells carrying a deletion of *COC*-associated *B-box* sequences. We propose that TFIIIC binding to the *B-box* sequences helps tether these loci to the nuclear periphery, thereby creating a barrier in the passage of processive heterochromatin complexes. As mentioned above, similar mechanisms are also believed to be essential for enhancer blocking activity of the insulator elements in *Drosophila* and in mammals, even though the proteins involved in the tethering process might be entirely different (Gerasimova et al., 2000; Yusufzai et al., 2004). Moreover, tethering of sequences to nuclear structures has been proposed to be important for barrier activity in *S. cerevisiae* (Ishii et al., 2002). These studies, along with our results, argue that insulators and boundary elements share a common mechanism to limit the range of action of enhancers and silencers, respectively, by tethering certain loci to subnuclear structures.

We found that the majority of *COC* sequences are located near the promoters of divergent genes. It is possible that *COC*s help separate independently regulated genes into distinct domains, preventing regulatory elements of a gene from affecting expression of another nearby gene. An additional function of *COC* might be to directly regulate the expression of nearby genes, which might be transcribed by either Pol II or Pol III. To this end, deletion of *B-boxes* severely affects transcription of *IR* elements. Intriguingly, one of the divergent Pol II promoter regions occupied by TFIIIC is the gene encoding Sfc3 (Figure 6), suggesting the potential for transcriptional autoregulation of TFIIIC. Besides regulating gene expression, the tethering of *COC* sites to the nuclear periphery might also have consequences for other chromosomal processes. For example, it has been shown that in *S. cerevisiae tRNA* genes act as DNA replication fork pause sites (Deshpande and Newlon, 1996). Likewise, the physical tethering of boundaries or *COC* sites to the nuclear periphery could inhibit the passage of replication fork, possibly dividing disparate chromosomal regions into autonomously replication domains. Furthermore, structural organization imposed by *COC*s and boundary elements might also have implications for maintenance of genomic integrity by prohibiting unwanted mitotic recombination.

How conserved is TFIIIC role in genome organization? In addition to the *tRNA*s, TFIIIC is known to bind to several sites across the *S. cerevisiae* genome independent of Pol III localization (Moqtaderi and Struhl, 2004). These sites, referred to as *ETC* loci, are perfectly conserved among different *Saccharomyces* species, leading to suggestions that these TFIIIC binding sites represent a new class of regulatory elements, but their exact function has not been defined. Similar to *COC* loci in fission yeast, *ETC* loci in budding yeast might have a role in genome organization via the tethering of specific chromosomal regions to subnuclear structures, akin to the clustering of *tRNA* genes near the nucleolus (Thompson et al., 2003). Indeed, our analysis showed that a subset of TFIIIC bodies seems to associate with the nucleolus, suggesting that in fission yeast *tRNA* genes might also be clustered in or around the nucleolus, and this higher-order organization could be involved in boundary activity of *tRNA* genes. In mammals, about 500,000 copies of *Alu* repeats that account for 5% of the genome content contain *B-box* sequences (Deininger, 1989), representing a large fraction of potential TFIIIC binding sites in spatial genome organization.

Therefore, the biological significance of the *COC* loci might be generally conserved among eukaryotes. Future studies that attempt to address the mechanism of TFIIIC-mediated tethering of specific loci to the nuclear periphery and the role of *COC* sites in the functional organization of the genome should lead to new insights into pathways governing complex chromosomal processes including gene regulation, DNA replication, and recombination.

EXPERIMENTAL PROCEDURES

Strain Constructions

Strains carrying *ura4*$^+$ inserted adjacent to the heterochromatin boundary or C-terminal Myc tagged Sfc6 were constructed using a PCR-based method (Bahler et al., 1998). The endogenous sequences were replaced with *kan*$^+$ gene to delete different portions of boundary elements. To generate *B-box*Δ strain, the DNA fragment lacking a 240-bp sequence consisting of five *B-boxes* was constructed by PCR. The strain carrying *kan*$^+$ at the *IR-R* region was transformed with the amplified PCR fragment, and G418-sensitive cells were selected. *B-box* deletion was confirmed by DNA sequencing. Because the deleted *COC3* region includes part of an essential gene, diploid cells were used to create the *COC3*Δ strain. One of the *COC3* alleles in wild-type diploid cells was replaced with *kan*$^+$ gene. All other strain constructions were performed using conventional genetic crosses.

ChIP Analysis

ChIP was carried out as described previously (Noma et al., 2001) except for analysis of the Pol III machinery binding, in which chromatin fixed with 3% paraformaldehyde followed by further cross-linking with 10 mM dimethyl adipimidate (DMA) was used to perform immunoprecipitations with previously described antibodies (Hamada et al., 2001). ChIP analysis for RNA pol II and histone H3 localization was done using anti-Pol II monoclonal antibody (8WG16, Covance) and anti-histone H3 polyclonal antibody (ab1791, Abcam), respectively. Genome-wide mapping of Sfc6 and Rpc130 was performed as previously described (Cam et al., 2005). Microarray data can be accessed at National Cancer Institute (http://pombe.nci.nih.gov/) and at NCBI GEO under the accession number GSE4555.

Heterochromatin-Spreading Assay

The spreading of heterochromatin into euchromatic regions was assayed using *ura4*$^+$ marker genes inserted at the right flank of the silent mating-type region and the left flank of *cen1*. Heterochromatin spreading onto the *ura4*$^+$ results in repression of the marker gene, thereby allowing cells to grow on 5-fluoroorotic acid (FOA) plates. To increase heterochromatin-spreading efficiency, *swi6*$^+$*-333* strains carrying three copies of *swi6*$^+$ genes at the endogenous locus were used. To ensure that no heterochromatin spreading had already occurred in starting cell colonies, cells expressing the *ura4*$^+$ genes were selected by replicating twice onto AA-URA plates prior to serial dilution analyses.

RNA Analysis

Total RNA was extracted from cells and analyzed by RT-PCR as described previously (Noma et al., 2004). Briefly, RNA (~10 μg) was treated with 10 units of DNase I (Promega) at 37°C for 30 min, and RNA samples (~250 ng) were subjected to RT-PCR (Onestep RT-PCR kit, Qiagen). To determine which strand is transcribed, first strand cDNA synthesis was performed with one primer complementary to either the forward or reverse transcripts, and a second primer was added before the PCR reaction. To ensure that no DNA contamination was present in the RNA sample, reverse transcriptase was omitted in (RT-) samples.

Microscopy Analysis

Immunofluorescence (IF) and fluorescent in situ hybridization (FISH) experiments were performed as described (Sadaie et al., 2003). To detect the Sfc3 protein by IF, a strain (yYH2230) with the endogenous *sfc3* gene replaced by an allele carrying the *nmt1*-driven Sfc3 N-terminal tagged with FLAG and His epitopes was used. This tagged Sfc3 protein is functional, and its association with other TFIIIC subunits in vivo was intact (Huang et al., 2000). Anti-FLAG M2 (Sigma-aldrich) and anti-Myc 9E10 monoclonal antibodies (Clontech Laboratories) were used to detect FLAG-Sfc3 and Sfc6-Myc (expressed under the control of native regulatory elements) proteins, respectively. FISH probes were generated using the cosmids, c336 (*COC3*), c1539 (*COC4*), c63 (*COC5*), c23G7 (the mating-type region), and the plasmid pRS140 (centromere).

Supplemental Data

Supplemental Data include four figures and one table and can be found with this article online at http://www.cell.com/cgi/content/full/125/5/859/DC1/.

ACKNOWLEDGMENTS

We thank J. Woodward for providing the cosmid clones and Y. Huang for a yeast strain and antibody. We also thank M. Lichten, R. Porter, and C. Denby for comments on the manuscript; T. Sugiyama, A. Guhathakurta, and R. Dhar for helpful discussions; and X. Chen for technical assistance. This research was supported by the Intramural Research Program of the NIH, National Cancer Institute, Center for Cancer Research.

Received: November 28, 2005
Revised: February 27, 2006
Accepted: April 3, 2006
Published: June 1, 2006

REFERENCES

Ayoub, N., Noma, K., Isaac, S., Kahan, T., Grewal, S.I., and Cohen, A. (2003). A novel jmjC domain protein modulates heterochromatization in fission yeast. Mol. Cell. Biol. *23*, 4356–4370.

Bahler, J., Wu, J.Q., Longtine, M.S., Shah, N.G., McKenzie, A., 3rd, Steever, A.B., Wach, A., Philippsen, P., and Pringle, J.R. (1998). Heterologous modules for efficient and versatile PCR-based gene targeting in Schizosaccharomyces pombe. Yeast *14*, 943–951.

Bell, A.C., and Felsenfeld, G. (2001). Insulators and boundaries: versatile regulatory elements in the eukaryotic genome. Science *291*, 447–450.

Bi, X., Yu, Q., Sandmeier, J.J., and Zou, Y. (2004). Formation of boundaries of transcriptionally silent chromatin by nucleosome-excluding structures. Mol. Cell. Biol. *24*, 2118–2131.

Blanton, J., Gaszner, M., and Schedl, P. (2003). Protein:protein interactions and the pairing of boundary elements in vivo. Genes Dev. *17*, 664–675.

Cam, H.P., Sugiyama, T., Chen, E.S., Chen, X., FitzGerald, P.C., and Grewal, S.I. (2005). Comprehensive analysis of heterochromatin- and RNAi-mediated epigenetic control of the fission yeast genome. Nat. Genet. *37*, 809–819.

Cavalli, G. (2002). Chromatin as a eukaryotic template of genetic information. Curr. Opin. Cell Biol. *14*, 269–278.

Deininger, P.L. (1989). SINEs: Short interspersed repeated DNA elements in higher eucaryotes. In Mobile DNA, D.E. Berg and M.M. Howe, eds. (Washington, DC: American Society for Microbiology), pp. 619–636.

Deshpande, A.M., and Newlon, C.S. (1996). DNA replication fork pause sites dependent on transcription. Science *272*, 1030–1033.

Donze, D., and Kamakaka, R.T. (2001). RNA polymerase III and RNA polymerase II promoter complexes are heterochromatin barriers in Saccharomyces cerevisiae. EMBO J. *20*, 520–531.

Gerasimova, T.I., Byrd, K., and Corces, V.G. (2000). A chromatin insulator determines the nuclear localization of DNA. Mol. Cell *6*, 1025–1035.

Grewal, S.I., and Moazed, D. (2003). Heterochromatin and epigenetic control of gene expression. Science *301*, 798–802.

Grunstein, M. (1998). Yeast heterochromatin: regulation of its assembly and inheritance by histones. Cell *93*, 325–328.

Hall, I.M., Shankaranarayana, G.D., Noma, K., Ayoub, N., Cohen, A., and Grewal, S.I. (2002). Establishment and maintenance of a heterochromatin domain. Science *297*, 2232–2237.

Hall, I.M., Noma, K., and Grewal, S.I. (2003). RNA interference machinery regulates chromosome dynamics during mitosis and meiosis in fission yeast. Proc. Natl. Acad. Sci. USA *100*, 193–198.

Hamada, M., Huang, Y., Lowe, T.M., and Maraia, R.J. (2001). Widespread use of TATA elements in the core promoters for RNA polymerases III, II, and I in fission yeast. Mol. Cell. Biol. *21*, 6870–6881.

Hsieh, Y.J., Kundu, T.K., Wang, Z., Kovelman, R., and Roeder, R.G. (1999). The TFIIIC90 subunit of TFIIIC interacts with multiple components of the RNA polymerase III machinery and contains a histone-specific acetyltransferase activity. Mol. Cell. Biol. *19*, 7697–7704.

Huang, Y., Hamada, M., and Maraia, R.J. (2000). Isolation and cloning of four subunits of a fission yeast TFIIIC complex that includes an ortholog of the human regulatory protein TFIIICbeta. J. Biol. Chem. *275*, 31480–31487.

Huang, Y., and Maraia, R.J. (2001). Comparison of the RNA polymerase III transcription machinery in Schizosaccharomyces pombe, Saccharomyces cerevisiae and human. Nucleic Acids Res. *29*, 2675–2690.

Ishii, K., Arib, G., Lin, C., Van Houwe, G., and Laemmli, U.K. (2002). Chromatin boundaries in budding yeast: the nuclear pore connection. Cell *109*, 551–562.

Jenuwein, T., and Allis, C.D. (2001). Translating the histone code. Science *293*, 1074–1080.

Jia, S., Noma, K., and Grewal, S.I. (2004). RNAi-independent heterochromatin nucleation by the stress-activated ATF/CREB family proteins. Science *304*, 1971–1976.

Kimura, A., Umehara, T., and Horikoshi, M. (2002). Chromosomal gradient of histone acetylation established by Sas2p and Sir2p functions as a shield against gene silencing. Nat. Genet. *32*, 370–377.

Kuhn, A.N., and Kaufer, N.F. (2003). Pre-mRNA splicing in Schizosaccharomyces pombe: regulatory role of a kinase conserved from fission yeast to mammals. Curr. Genet. *42*, 241–251.

Labrador, M., and Corces, V.G. (2002). Setting the boundaries of chromatin domains and nuclear organization. Cell *111*, 151–154.

Litt, M.D., Simpson, M., Gaszner, M., Allis, C.D., and Felsenfeld, G. (2001). Correlation between histone lysine methylation and developmental changes at the chicken beta-globin locus. Science *293*, 2453–2455.

Meneghini, M.D., Wu, M., and Madhani, H.D. (2003). Conserved histone variant H2A.Z protects euchromatin from the ectopic spread of silent heterochromatin. Cell *112*, 725–736.

Moqtaderi, Z., and Struhl, K. (2004). Genome-wide occupancy profile of the RNA polymerase III machinery in Saccharomyces cerevisiae reveals loci with incomplete transcription complexes. Mol. Cell. Biol. *24*, 4118–4127.

Noma, K., Allis, C.D., and Grewal, S.I. (2001). Transitions in distinct histone H3 methylation patterns at the heterochromatin domain boundaries. Science *293*, 1150–1155.

Noma, K., Sugiyama, T., Cam, H., Verdel, A., Zofall, M., Jia, S., Moazed, D., and Grewal, S.I. (2004). RITS acts in cis to promote RNA interference-mediated transcriptional and post-transcriptional silencing. Nat. Genet. *36*, 1174–1180.

Oki, M., and Kamakaka, R.T. (2005). Barrier function at HMR. Mol. Cell *19*, 707–716.

Partridge, J.F., Borgstrom, B., and Allshire, R.C. (2000). Distinct protein interaction domains and protein spreading in a complex centromere. Genes Dev. *14*, 783–791.

Paule, M.R., and White, R.J. (2000). Survey and summary: transcription by RNA polymerases I and III. Nucleic Acids Res. *28*, 1283–1298.

Recillas-Targa, F., Pikaart, M.J., Burgess-Beusse, B., Bell, A.C., Litt, M.D., West, A.G., Gaszner, M., and Felsenfeld, G. (2002). Position-effect protection and enhancer blocking by the chicken beta-globin insulator are separable activities. Proc. Natl. Acad. Sci. USA *99*, 6883–6888.

Roberts, D.N., Stewart, A.J., Huff, J.T., and Cairns, B.R. (2003). The RNA polymerase III transcriptome revealed by genome-wide localization and activity-occupancy relationships. Proc. Natl. Acad. Sci. USA *100*, 14695–14700.

Rustici, G., Mata, J., Kivinen, K., Lio, P., Penkett, C.J., Burns, G., Hayles, J., Brazma, A., Nurse, P., and Bahler, J. (2004). Periodic gene expression program of the fission yeast cell cycle. Nat. Genet. *36*, 809–817.

Sadaie, M., Naito, T., and Ishikawa, F. (2003). Stable inheritance of telomere chromatin structure and function in the absence of telomeric repeats. Genes Dev. *17*, 2271–2282.

Scott, K.C., Merrett, S.L., and Willard, H.F. (2006). A heterochromatin barrier partitions the fission yeast centromere into discrete chromatin domains. Curr. Biol. *16*, 119–129.

Sugiyama, T., Cam, H., Verdel, A., Moazed, D., and Grewal, S.I. (2005). RNA-dependent RNA polymerase is an essential component of a self-enforcing loop coupling heterochromatin assembly to siRNA production. Proc. Natl. Acad. Sci. USA *102*, 152–157.

Suka, N., Luo, K., and Grunstein, M. (2002). Sir2p and Sas2p opposingly regulate acetylation of yeast histone H4 lysine16 and spreading of heterochromatin. Nat. Genet. *32*, 378–383.

Sun, F.L., and Elgin, S.C. (1999). Putting boundaries on silence. Cell *99*, 459–462.

Thompson, M., Haeusler, R.A., Good, P.D., and Engelke, D.R. (2003). Nucleolar clustering of dispersed tRNA genes. Science *302*, 1399–1401.

Thon, G., Bjerling, P., Bunner, C.M., and Verhein-Hansen, J. (2002). Expression-state boundaries in the mating-type region of fission yeast. Genetics *161*, 611–622.

Weinmann, R., and Roeder, R.G. (1974). Role of DNA-dependent RNA polymerase 3 in the transcription of the tRNA and 5S RNA genes. Proc. Natl. Acad. Sci. USA *71*, 1790–1794.

West, A.G., Huang, S., Gaszner, M., Litt, M.D., and Felsenfeld, G. (2004). Recruitment of histone modifications by USF proteins at a vertebrate barrier element. Mol. Cell *16*, 453–463.

Wood, V., Gwilliam, R., Rajandream, M.A., Lyne, M., Lyne, R., Stewart, A., Sgouros, J., Peat, N., Hayles, J., Baker, S., et al. (2002). The genome sequence of *Schizosaccharomyces pombe*. Nature *415*, 871–880.

Yamada, T., Fischle, W., Sugiyama, T., Allis, C.D., and Grewal, S.I. (2005). The nucleation and maintenance of heterochromatin by a histone deacetylase in fission yeast. Mol. Cell *20*, 173–185.

Yusufzai, T.M., Tagami, H., Nakatani, Y., and Felsenfeld, G. (2004). CTCF tethers an insulator to subnuclear sites, suggesting shared insulator mechanisms across species. Mol. Cell *13*, 291–298.